NRC Research Press

ARTICLE

Description of cochlear morphology and hair cell variation in the beluga whale[1]

Cassandra D. Girdlestone, Marina A. Piscitelli-Doshkov, Sonja K. Ostertag, Maria Morell, and Robert E. Shadwick

Abstract: Environmental change and decreased ice cover in the Arctic make new areas accessible to humans and animals. It is important to understand how these changes impact marine mammals, such as beluga whales (*Delphinapterus leucas* Pallas, 1776). Hearing is crucial in the daily lives of cetaceans. Consequently, we need normal baselines to further understand how anthropogenic noise affects these animals. Relatively little is known about the inner ear morphology of belugas, particularly the organ of Corti, or hearing organ, found within the cochlea. The base of the cochlea encodes for high-frequency sounds, while low frequencies are detected in the apex. We showed differences between the apex, or centremost point of the cochlea, and the base, the region closest to the stapes. Our results showed that average outer hair cell density changed from 148 cells/mm in the apex to 117 cells/mm in the base. Cell width varied between the two regions, from 5.8 μm in the apex to 8.4 μm in the base. These results revealed variation throughout the cochlea, and thus the need to understand the basic morphology, to give further insight on hearing function in belugas and allow us to recognize damage if or when we find it.

Key words: Beluga (*Delphinapterus leucas*), cochlea, inner ear, odontocetes, organ of Corti.

Résumé : Le changement de l'environnement et la diminution de la couverture de glace dans l'Arctique donnent lieu à de nouvelles zones accessibles aux humains et aux animaux. Il est important de comprendre comment ces changements influent sur les mammifères marins, comme les bélugas (*Delphinapterus leucas* Pallas, 1776). L'ouïe est primordiale dans la vie quotidienne des cétacés. Par conséquent, nous avons besoin de conditions de base normales afin de comprendre davantage comment le bruit anthropique affecte ces animaux. On en sait relativement peu sur la morphologie de l'oreille interne de bélugas, particulièrement l'organe de Corti, ou organe d'audition, situé dans la cochlée. La base de la cochlée code les sons aigus, tandis que les sons graves sont détectés au niveau de l'apex. Nous avons montré les différences entre l'apex, soit le point le plus au centre de la cochlée et la base, la région la plus proche de l'étrier. Nos résultats ont indiqué que la densité moyenne de cellules de poil extérieur variait de 148 cellules/mm dans l'apex à 117 cellules/mm dans la base. La largeur de cellule variait entre les deux régions, de 5,8 μm dans l'apex à 8,4 μm dans la base. Ces résultats ont révélé de la

Received 30 June 2017. Accepted 27 September 2017.

C.D. Girdlestone, M.A. Piscitelli-Doshkov, and R.E. Shadwick. Department of Zoology, University of British Columbia, Vancouver, BC V6T 1Z4, Canada.
S.K. Ostertag. Fisheries and Oceans Canada, Freshwater Institute, Winnipeg, MB R3T 2N6, Canada.
M. Morell. Department of Zoology, University of British Columbia, Vancouver, BC V6T 1Z4, Canada; INSERM-UMR 1051, Institute for Neurosciences of Montpellier, 34091 Montpellier, France.
Corresponding author: C.D. Girdlestone (e-mail: cassgird@zoology.ubc.ca).
[1]This article is part of a Special issue entitled "The beluga summit: knowledge sharing of the eastern Beaufort Sea beluga whale".

variation partout dans la cochlée et ainsi la nécessité de comprendre la morphologie de base afin de donner un nouvel aperçu de la fonction de l'ouïe chez les bélugas et nous permettre de reconnaître des dommages si ou quand nous les trouvons. [Traduit par la Rédaction]

Mots-clés : béluga (*Delphinapterus leucas*), cochlée, oreille interne, odontocêtes, organe de Corti.

Introduction

Ice cover in the Arctic is decreasing (Lei et al. 2015) and, as a result, additional areas of the ocean, previously difficult to reach, are becoming more accessible to both humans and animals. This opening up of seaways is expected to result in increased shipping traffic, seismic oil exploration, and other anthropogenic activities, which will in turn result in alterations in the Arctic soundscape. Decreased ice cover can also factor into these changes, as the presence of ice can act as a barrier, preventing sounds transmitted in the air from entering the ocean (Roth 2008). It is important to consider how this is affecting populations of marine life, including marine mammals such as beluga whales (*Delphinapterus leucas* Pallas, 1776). To understand future impacts, we need to understand the current health status of these animals. With regard to the beluga whale, a species that is completely dependent on its hearing for all aspects of daily life, we need to understand the morphology of their inner ear to recognize hearing damage or acoustic trauma if, or when, we find it.

Within the inner ear is a spiral-shaped structure known as the cochlea (Fig. 1A). The cochlea is comprised of three fluid-filled ducts, or channels. The centremost of these channels is where the organ of Corti, the hearing organ, is located (Fig. 1B). The surface of the organ of Corti (Fig. 1C) reveals an arrangement of cells wherein the inner hair cells (IHCs) are organized in a single row, while the outer hair cells (OHCs) form three parallel rows (Lim 1986). The IHCs and OHCs are the sensory cells of the organ of Corti. OHCs play a crucial role in frequency selectivity and increasing sensitivity, while IHCs are the true auditory cells, responsible for the transduction of the mechanical stimulus into an electrical signal (for a review, see Fettiplace and Kim 2014). The organization of certain structures within the inner ear is well documented in terrestrial mammals, pinnipeds, and some cetaceans (Wever et al. 1971*a*, 1971*b*, 1972; Lim 1986; Ketten and Wartzok 1990; Gao and Zhou 1992; Roth and Bruns 1992; Wartzok and Ketten 1999; Morell et al. 2015). Some of the features already described for various odontocetes, or toothed whales, include the length, thickness, and width of the basilar membrane, density of cells in the cochlea, and information about the ganglion cells and nerves. However, with regard to beluga whales, there is an absence of any general description of the morphology of the organ of Corti. Much of the currently ongoing work reflects the importance of understanding beluga hearing — their hearing range and acuity, behavioural effects of anthropogenic sound, and the mechanisms involved in sound production and reception used for echolocation (Wartzok et al. 2003; Castellote et al. 2014). We are particularly interested in the reception of sound and how the hair cells and their morphometrics relate to their hearing ability. However, it is also important to understand what normal baselines and their basic morphology consist of to further understand other aspects of beluga hearing. This paper describes morphological features of the beluga whale inner ear, specifically the hair cells of the organ of Corti. In addition to this, recommended methods of fixation and decalcification are addressed to further enable the successful analysis of cochlear samples for this and other species of marine mammals.

Fig. 1. Schematics and image of the location of the cochlea and the organ of Corti. (A) Beluga cochlea; image taken with a dissecting microscope. Arrows indicate the maximum and minimum distances between the outer edges of the spiral ligament used to calculate the cochlear diameter. (B) Schematic of the cochlea showing the location of the organ of Corti (OpenStax image adapted from https://upload.wikimedia.org/wikipedia/commons/1/1c/1406_Cochlea.jpg in accordance with licensing: https://creativecommons.org/licenses/by/4.0/legalcode). (C) Scanning electron micrograph of the surface of the organ of Corti in a beluga cochlea showing the typical arrangement of the hair cells. Visible here is the single row of inner hair cells (IHC) as well as the three parallel rows of outer hair cells (OHC1, OHC2, and OHC3). Each "U" or "W" shape represents one hair cell. Measurements shown are (*i*) IHC width, (*ii*) distance from IHC to the third row of OHCs, and (*iii*) OHC width.

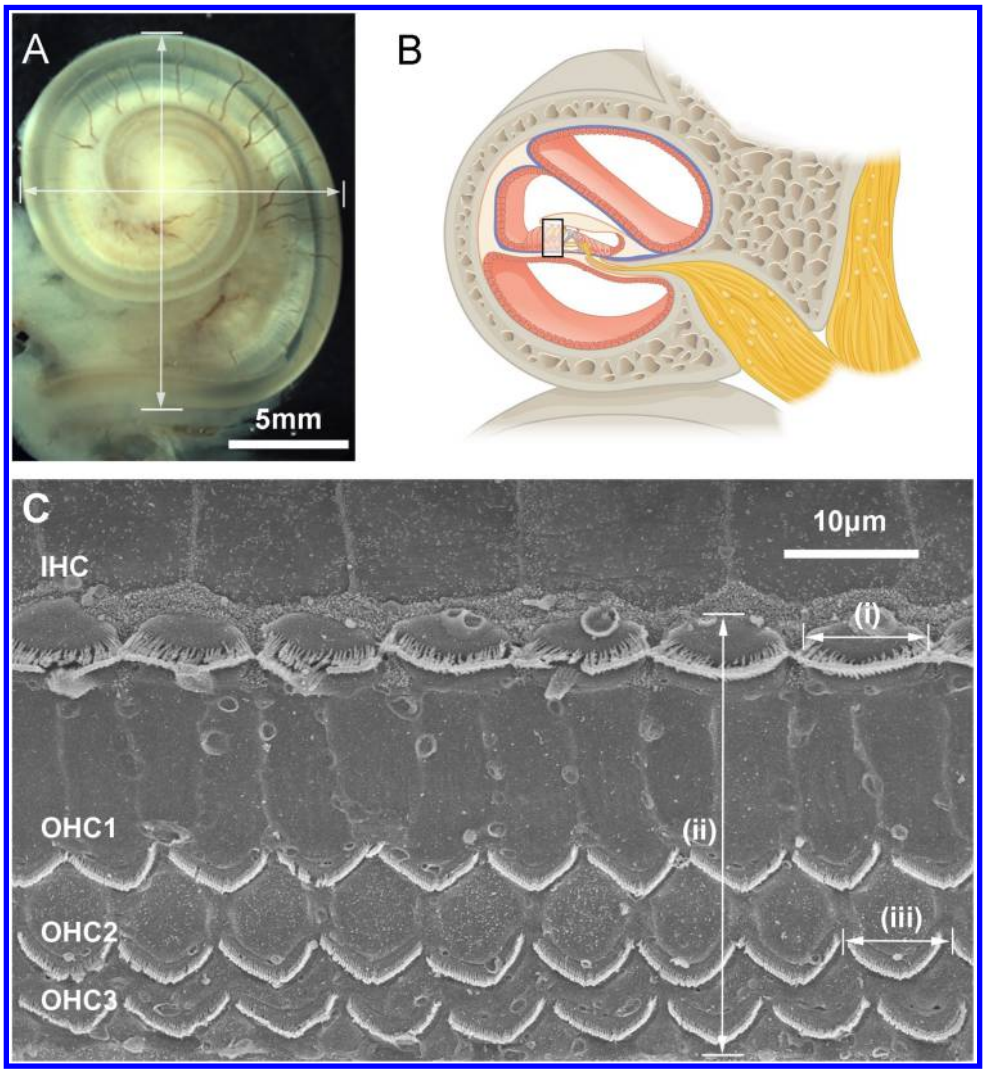

Materials and methods

Extraction and fixation

Beluga whale ear samples (right and left) were collected from four individuals ($n = 8$), harvested in 2014 at Hendrickson Island, Northwest Territories, Canada, as part of subsistence harvesting. Prior to the start of the sampling season, all required permits were obtained as follows: Aurora Research Institute (ARI) licence No. 15467, Department of

Fisheries and Oceans (DFO) fishing licence No. S-14/15-3019-YK, Marine Mammal Transport licence No. 18843, and Environmental Impact Screening Committee (EISC) No. 03-14-03.

Ear samples were extracted in the field and fixed within 1.5–5 h post-mortem for each individual (Supplementary Table S1[1]). The shorter the window of time post-mortem, in which the samples are fixed, the better, to minimize deterioration. Fresh samples such as these can in turn yield more reliable results than samples collected opportunistically and in varying, unknown stages of decomposition. Samples were extracted and subsequently fixed using one of three solutions: 10% neutral buffered formalin (NBF) or 2.5% glutaraldehyde in 0.1 mol/L phosphate buffer (pH 7.4) or alternatively 2.5% glutaraldehyde in 0.1 mol/L cacodylate buffer (pH 7.3) according to the protocol by Morell and André (2009). Once the ear samples were fixed, they were shipped for further laboratory analysis to the University of British Columbia, Vancouver, British Columbia, Canada.

Decalcification

Following fixation of the samples, the periotic bone that surrounds the cochlea was decalcified. Decalcification was only required to the point at which the vestibular scala and the stria vascularis were visible. This was done using one of two treatment options (Supplementary Table S1[1]). The first solution used was 14% ethylenediaminetetraacetic acid (EDTA) tetrasodium salt (pH 7.4) as described by Morell et al. (2015, 2017). A second solution that was used on some of the samples was RDO® (Apex Engineering Products, Aurora, Illinois, USA), a rapid decalcifier. Decalcification was achieved by initially placing the sample in 50% RDO® (diluted with distilled water) for 24 h, at which point the sample was moved to 25% RDO® (diluted with distilled water) as described in Morell et al. (2009).

Scanning electron microscopy: dissection and processing

Once the cochlear samples were suitably decalcified, they were dissected with the vestibular scala and the stria vascularis sectioned and both Reissner's membrane and the tectorial membrane removed. Samples were then dehydrated using ethanol, gradually increasing the concentration until reaching 100%. Once dehydrated, the cochlear samples were critical point dried using CO_2 and sputter coated with either gold–palladium or platinum–palladium in preparation for imaging in a Hitachi S-4700 scanning electron microscope (SEM) at the University of British Columbia Bioimaging Facility, Vancouver, British Columbia, Canada.

Image analysis and morphometry

SEM micrographs were adjusted for brightness and contrast using Adobe Photoshop® CS3. Measurements of the cochlear structures were made using ImageJ® software.

Since the shape of the entire cochlea is more ovoid than round, there is both a minimum and a maximum diameter (i.e., minimum and maximum distance between the outer margins of the spiral ligament) (Fig. 1A). The cochlear diameter was calculated by taking the mean of these two measurements for each cochlea.

Cochlear length was measured at the level of the limit between the first row of OHCs and inner pillar cells using an average of 85 flat SEM micrographs per each ear. The length to be measured in each image was delineated prior to measuring to ensure an accurate length with no overlap or gaps.

The average number of hair cells per 100 μm was calculated for each of the apex, middle, and base regions of the cochlear samples. For the purposes of this paper, the apex region

[1]Supplementary data are available with the article through the journal Web site at http://nrcresearchpress.com/doi/suppl/10.1139/as-2017-0031.

Fig. 2. Scanning electron micrographs showing fixation using (A) 10% neutral buffered formalin and (B) 2.5% glutaraldehyde in 0.1 mol/L cacodylate buffer, pH 7.3.

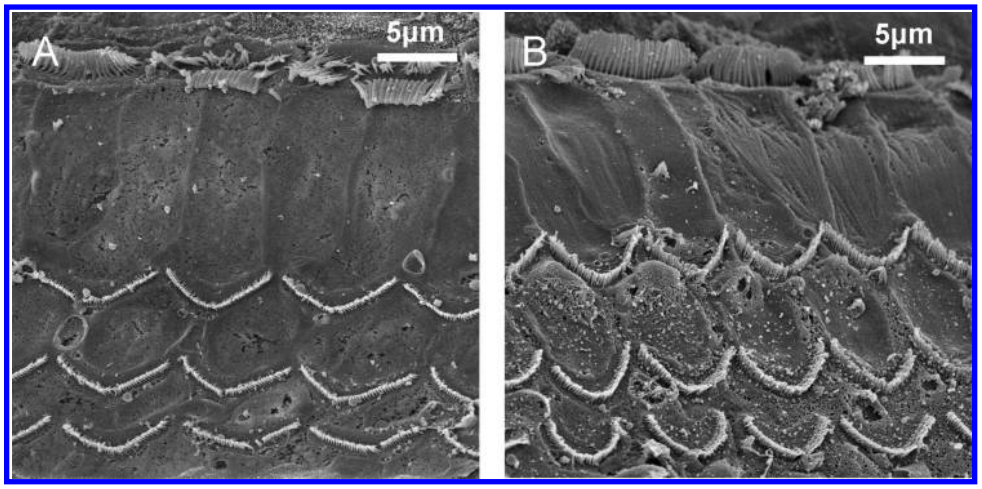

was defined as the first 33% of the cochlear length (closest to the inner point of the cochlea). The middle region refers to the next 33%–66% and the base region to the last 34% of the cochlear length. These averages were then used to extrapolate the total number of hair cells (both outer and inner) per cochlea.

Both the area and cell width measurements were calculated using ImageJ® (Fig. 1C). The distance between the IHCs and third row of OHCs was also measured and compared among all three regions.

Results

Several methods of fixation and decalcification were examined to further enable the successful analysis of cochlear samples for this and other species of marine mammals. During the fixation process, when 10% NBF was used, the end quality of the samples was comparable with those fixed with 2.5% glutaraldehyde (Fig. 2). In the one beluga in our study, for which one ear was treated with EDTA and the other with RDO®, we found that the cochlea that was decalcified with EDTA was slightly better preserved (Fig. 3).

Cochlear samples of both ears from four adult beluga whales ($n = 8$) were analyzed to determine the cochlear diameter, cochlear turns, total cochlear length, and hair cell count as well as to compare any variation in the width of the hair cells between the apex, middle, and base regions of each cochlea. The comparisons measured the density of the OHCs, cell width for both the IHCs and OHCs, and the distance between the IHCs and third row of OHCs.

The average cochlear diameter was determined to be 14.6 mm. The samples in this study all had two cochlear turns. The mean cochlear length (measured along the limit between the first row of OHCs and the inner pillar cells) for these samples was calculated to be 41.3 mm, with a range of 39.5–42.6 mm. In addition to examining the whole cochlea, we compared the hair cells of the apex, or centremost point of the cochlea, with those in the middle section and the base, or outermost area of the cochlea, closest to the stapes. The cells sampled were from these three regions, each of which covered a distance of 33% of the cochlear length. There was some degree of variation in the cells of the three regions (Fig. 4) as well as variation even within the apex region (Figs. 4A and 4B).

Fig. 3. Scanning electron micrographs of beluga cochleas decalcified using (A) EDTA and (B) RDO®.

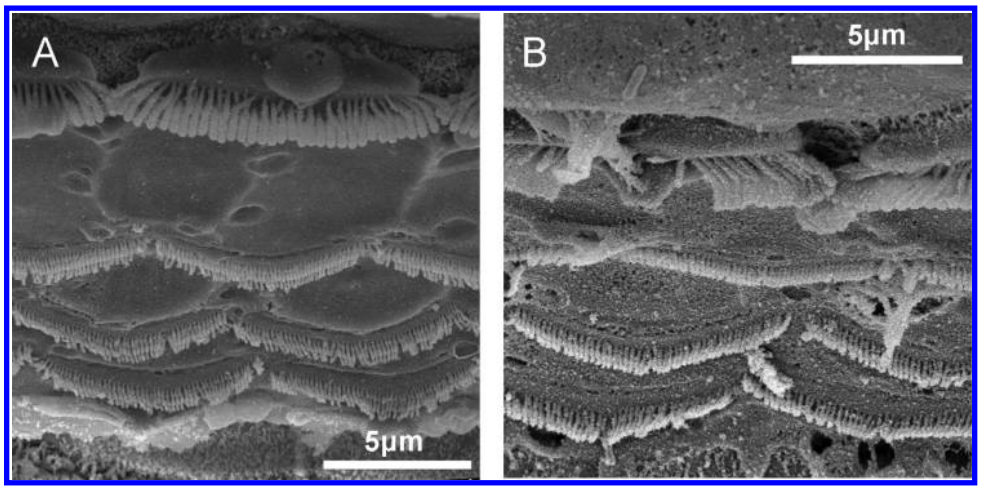

In the apex, the mean cell width of IHCs was found to be 8.0 µm, while the mean width of the OHCs was 5.8 µm (Table 1). The mean cell widths were similar among the three rows of OHCs, ranging from 5.3 to 6.0 µm (Fig. 5). In comparison, the IHCs had a mean width of 9.7 µm in the middle region of the cochlea. The mean of the OHCs in this region was 8.6 µm, with the mean ranging from 8.4 to 8.7 µm. Similarly to the middle region, the IHCs of the base region had a mean width of 9.7 µm. While again comparable with the cells in the middle region, but in contrast with the cells in the apex region, the mean width of the OHCs in the base was 8.4 µm, the mean ranging from 8.2 to 8.5 µm. The distance between the IHCs and third row of OHCs showed a decrease of 19 µm moving from the apex to the base (Fig. 6).

Hair cell density between the apex and base was also examined for all four rows (Fig. 7). The mean of the measurements for the hair cells in the apex showed a cell density of 148 cells/mm, while in the middle and base regions, the cell density was the same at 117 cells/mm. The total number of hair cells per cochlea, averaged among samples, was calculated as a range of 2384–5494 IHCs and 7151–21 695 OHCs (or approximately 2384–7232 OHCs in each of the three rows). These wide ranges were calculated using the absolute minimum and maximum cell counts per millimetre of cochlear length in all three regions combined. This was due to the fact that the cell density is not equal among regions or throughout the length of the cochlea.

Discussion

The goal of this research was twofold: to determine how to best process cochlear samples to preserve their quality, especially in field conditions, and to examine the morphology of the inner ear of the beluga whale.

High-quality samples are essential to analyze cochlear samples and obtain reliable results about the morphometry and structures present. For sample fixation, since we obtained similar results with all fixative solutions, the use of 10% NBF is recommended, as it is widely available and effective for fixing samples (Fig. 2). The benefits of 10% NBF for stranding networks worldwide are its easy accessibility, it is already in use for the fixation of all other organs, and it has a lower toxicity than glutaraldehyde.

Fig. 4. Examples of the variation in the morphology of the hair cells from the beluga whale cochlea and showing (A and B) hair cells from two locations within the apex region (33% distance from the apex), (C) hair cells in the middle region (located in the range of 33%–66% of the cochlear length from the apex), and (D) the base region (the last 34% of the cochlea).

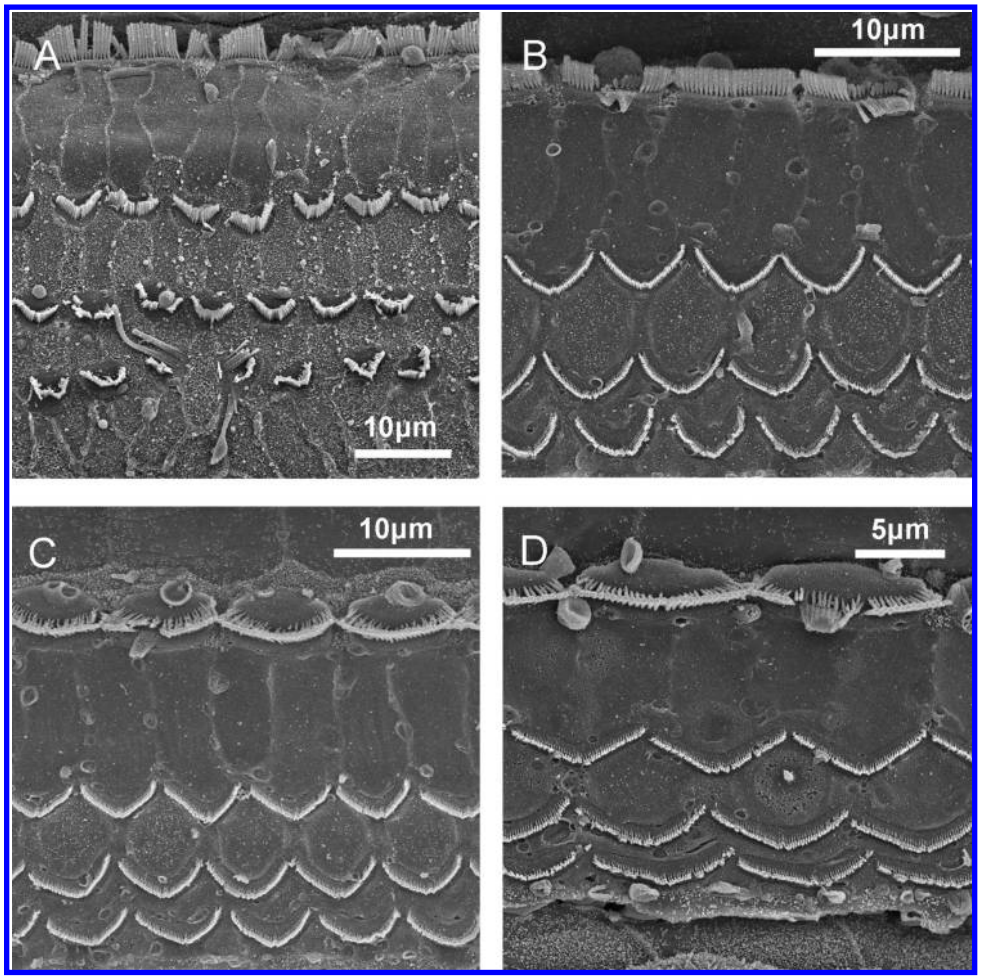

The dehydration process, using 90%–100% ethanol, required for viewing samples in the SEM can result in tissue shrinkage of the sample compared with a sample in a fresh state (Edge et al. 1998). The amount of shrinkage that occurs when using formaldehyde has been documented as not being statistically significant (Edge et al. 1998). Since we expect the shrinkage of the organ of Corti and potential distortion of the structures due to fixation to be homogeneous throughout the spiral (Yarin et al. 2014), the shape of its cells would be largely preserved.

We recommend EDTA as our preferred solution for decalcifying samples, recognizing that the process is longer yet yields slightly higher quality results (Fig. 3). It also preserves the quality of the soft tissue in the cochlea, which is crucial when examining fine structures and cell morphology. Our sample size was too small to say definitively if there was a difference in the beluga ear samples, as only one individual had decalcification done using different solutions on each ear. However, this result was confirmed in previous studies on other species of cetaceans, where there was either no difference or EDTA was slightly better

Table 1. Beluga whale mean cochlear measurements (± standard deviation) comparing the inner hair cells (IHCs) and outer hair cells (OHCs) from the apex, middle, and base regions using scanning electron microscopy.

		General location					
		Apex		Middle		Base	
Measurement	*n*	Range	Mean	Range	Mean	Range	Mean
IHC count	36	87–136	111±14	85–104	93±7	59–118	88±21
Total number of IHCs (whole cochlea)	36			2384–5494			
OHC1 count	41	114–179	151±21	104–132	117±9	71–156	117±31
OHC2 count	41	118–179	150±20	104–132	117±9	71–156	117±31
OHC3 count	41	59–179	143±27	102–132	116±10	71–156	117±31
Total number of OHCs (per row)	41			2384–7232			
Total number of OHCs (whole cochlea)	41			7151–21 695			
IHC width (μm)	175	6.0–9.8	8.0±0.9	8.0–11.8	9.7±1.0	7.1–12.0	9.7±1.3
OHC1 width (μm)	241	4.0–7.6	6.0±0.7	7.4–10.5	8.7±0.7	6.5–10.4	8.5±1.1
OHC2 width (μm)	227	4.1–8.5	5.9±0.9	7.1–10.1	8.6±0.7	6.1–10.2	8.3±1.2
OHC3 width (μm)	200	3.7–7.2	5.3±0.8	6.3–10.8	8.4±1.0	6.5–9.2	8.2±0.8
Mean OHC width (μm)	668		5.8±0.8		8.6±0.8		8.4±1.1
IHC–OHC3 distance (μm)	131	21.8–41.8	34.7±3.9	15.0–27.7	22.9±4.3	15.2–16.4	15.7±0.6

Note: Cell counts are measured in cells/mm; mean cochlear length was 41.3 mm.

Fig. 5. Beluga whale mean hair cell width±standard deviation of the inner hair cells (IHC) and outer hair cells (OHC) in each of the corresponding regions (apex, middle, and base) within the cochlea.

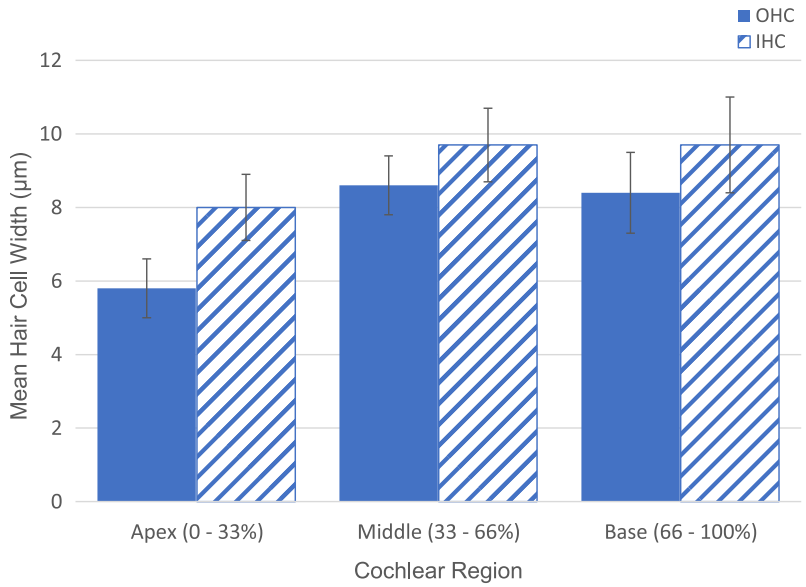

(M. Morell, unpublished data). When the results from analyzing a particular sample are required in a timelier manner, we recommend the use of RDO®, which is a rapid decalcifying agent. If lesions, indicative of noise-induced hearing loss (or hearing impairment due to other etiologies), are present, they can still be detected when either EDTA or RDO® is used. Maintaining sample quality is essential for determining more accurately the importance and the function of both cochlear structures and morphometrics.

Fig. 6. Beluga whale mean distance±standard deviation from the inner hair cells (IHC) to the third row of outer hair cells (OHC3) in each of the corresponding regions (apex, middle, and base) within the cochlea.

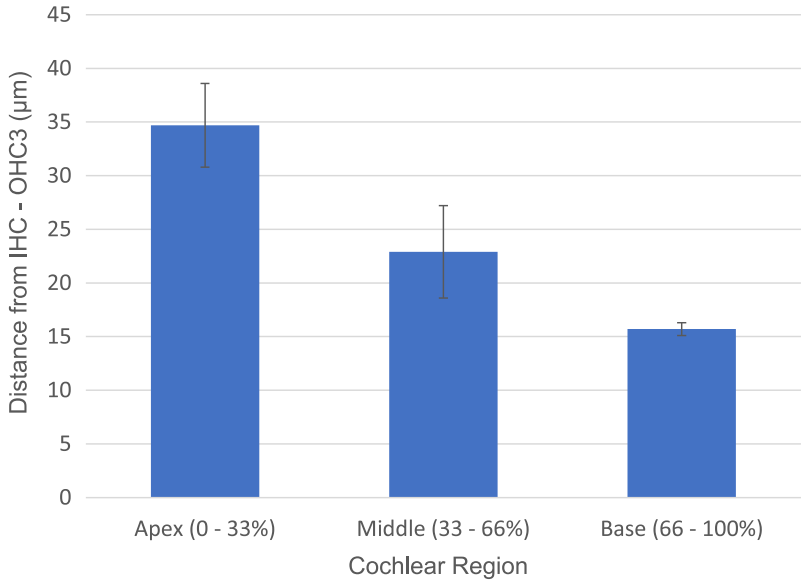

Fig. 7. Beluga whale mean hair cell density of the inner hair cells (IHC) and outer hair cells (OHC) in each of the corresponding regions (apex, middle, and base) within the cochlea.

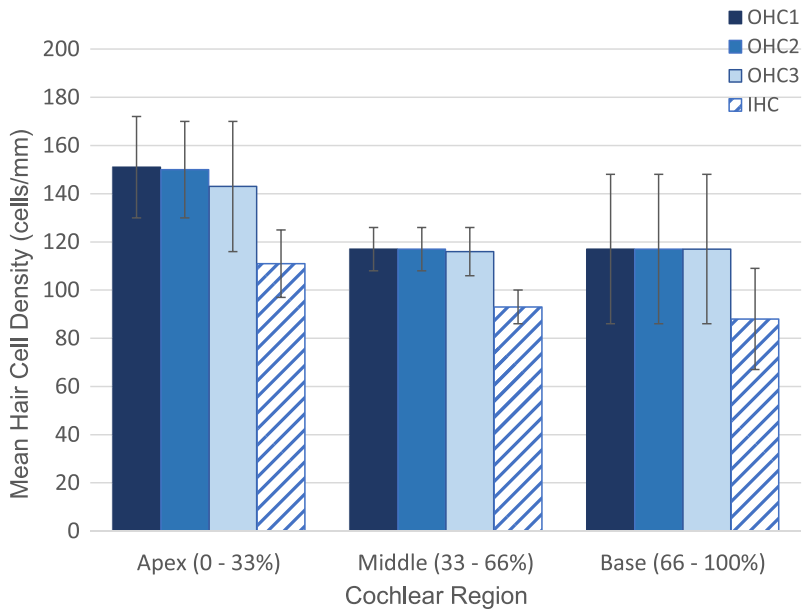

We examined the basic structural organization to identify normal baselines and to help us understand how anthropogenic activities and the changing environment might impact beluga whales. Understanding the morphology of normal ears in beluga whales is essential for recognizing pathology or damage if or when it is detected.

As in other terrestrial and marine mammals, the standard cellular arrangement of a single row of IHCs and three parallel rows of OHCs was present in each cochlea. The mean length of the beluga cochleas that we examined (41 mm) was comparable with the basilar membrane length (42 mm) of beluga cochleas described by Ketten (2000). The length of the cochlea, but not the width, typically exhibits a positive correlation with body size, although this relationship is not as strong in the beluga as it is in other mammals (Ketten 1992*a*).

The number of cochlear turns varies among species of odontocetes and can range from 1.5 up to 2.5 turns (Ketten and Wartzok 1990; Ketten 1992*a*; Solntseva 2010). The number of turns found in our samples was two, which corresponds to previous work by Sensor et al. (2015) in which they found 1.75–2 turns in the ears of beluga whales. Ketten and Wartzok (1990) categorized marine species as specialists with two distinct cochlear morphologies, separated into Type I (high frequency) and Type II (low frequency) (reviewed in Ketten 1992*a*, 1992*b*). Under this distinction, beluga whales are classified as Type II odontocetes.

Hair cell density and counts have not been previously discussed for beluga whales. Instead, earlier work describes the density and counts of the spiral ganglion cells or afferent neuron cell body counts (Gao and Zhou 1992; Ketten 2000; Sensor et al. 2015). In our study, the total number of hair cells (inner and outer combined) was conservatively calculated to be 9535–28 927 based on absolute minimum and maximum counts. The average number of IHCs calculated in our beluga samples was 3939±1555, while the average for the OHCs was 14 423±7272. The range of these measurements is large due to the variability in cochlear length among individuals as well as sensory cell density in the apex, middle, and base (Table 1). These counts are similar to the hair cell counts for the bottlenose dolphin (*Tursiops truncatus* Montagu, 1821) by Wever et al. (1971*b*) in which they found 3451 IHCs and 13 923 OHCs in cochleas of similar length (38.5 mm). In addition to interspecies variation, it is also important to consider intraspecies or interindividual variation. Our range is conservative, since it was calculated based on minimum versus the maximum potential total number of hair cells, both inner and outer. It is difficult to calculate the interindividual variation of hair cell counts for beluga based on our sample size. However, this research provides a first estimate based on differential hair cell density along the cochlear spiral.

While we did not examine spiral ganglion cell counts, they have been calculated for many species of cetaceans and show a wide range across species, from 68 000 to >168 000 (Ketten 1997). Spiral ganglion cells in cetaceans are much greater in number than in land mammals of comparable cochlear length, which is likely correlated with a greater complexity of information processed by the neurons during echolocation (Ketten and Wartzok 1990).

The OHC width in the apex, measured by Morell et al. (2015) in other odontocete species, was found to range from 5.04 to 5.6 μm in the striped dolphin (*Stenella coeruleoalba* Meyen, 1833) and from 5.47 to 6.2 μm in the harbour porpoise (*Phocoena phocoena* Linnaeus, 1758) and were of the same magnitude as in the beluga. This morphological variation shows that there is indeed some individual variation within a species but also that there are similarities among related species. In our study, we also show a greater width of the organ of Corti at the apex compared with the base of the cochlea. In addition, there was also a measurable decrease in hair cell density towards the base of the cochlea, as a direct result of the increased cell width. There is a tonotopic distribution of the organ of Corti along the cochlear spiral in mammals. The apex of the cochlea is where lower frequencies are encoded, while the base of the cochlea is where high frequencies are encoded. The frequencies that are encoded in a particular region depend on the stiffness of the basilar membrane (Von Békésy 1960; Dong and Olson 2009). However, other studies from terrestrial mammals show

a relationship between the coding frequency and other structures such as the length of the OHC body (Dannhof et al. 1991; Pujol et al. 1992), cross-sectional area of the organ of Corti cells (Schweitzer et al. 1996), ultrastructure of supporting cells (Spicer and Schulte 1994), or morphometrics of the reticular lamina (Yarin et al. 2014). The morphometrics measured here for sensory cells and the distance between the IHCs and third row of OHCs in the apex of the beluga (Table 1; Figs. 5 and 6) are consistent with those of guinea pig measured from SEM micrographs (Yarin et al. 2014). In the case of the guinea pig, it is well described how several morphometrics of the reticular lamina of the organ of Corti change through the cochlear spiral and how this relates to their frequency map. Our measurements of the apex are of the same magnitude as those found by Yarin et al. (2014). This can be explained by the fact that the hearing range of guinea pig extends up to 30 kHz (Tsuji and Liberman 1997), while beluga whales can hear up to 150 kHz (Castellote et al. 2014). Thus, having information on hair cell morphometrics is necessary for understanding how morphology relates to hearing function specific to each species. Mechanics of the organ of Corti are relatively well described (Chen et al. 2011; Liu et al. 2015; Soons et al. 2015; Lee et al. 2016; Ni et al. 2016). However, if the morphometrics of the reticular lamina are consistent among species, this may have some biomechanical implications.

Conclusion

The study of the morphology and structural changes in cetacean inner ears, specifically beluga whales, lacks description and is of increasing importance. To our knowledge, this study is the first to describe the morphological variation of the organ of Corti between the apex, middle, and base of the cochlea in the inner ear of the beluga whale. There is a distinct decrease in hair cell density and increase in hair cell width as we move from the apex to the base. This indicates, as in other mammalian species, that there are trends in the morphology and morphometrics associated with various locations in the cochlea.

Gaining knowledge of the basic morphology can provide us with an understanding of normal baselines, which can further aid us in determining potential impacts and effects of human-made noise on marine mammals such as beluga whales.

Acknowledgements

Thank you to the following agencies from which the required permits were obtained: ARI, DFO, and EISC. The authors would also like to thank Lisa Loseto (DFO, Canada), Stephen Raverty (British Columbia Ministry of Agriculture and Lands), and for technical help Derrick Horne (Bioimaging Facility, University of British Columbia). We especially thank the Tuktoyaktuk community hunters and the Tuktoyaktuk Hunters and Trappers Committee, who supported and approved this sampling and research.

References

Castellote, M., Mooney, A.T., Quakenbush, L., Hobbs, R., Goertz, C., and Gaglione, E. 2014. Baseline hearing abilities and variability in wild beluga whales (*Delphinapterus leucas*). J. Exp. Biol. **217**: 1682–1691. doi: 10.1242/jeb.093252. PMID: 24829324.

Chen, F., Zha, D., Fridberger, A., Zheng, J., Choudhury, N., Jacques, S.L., Wang, R.K., Shi, X., and Nuttall, A.L. 2011. A differentially amplified motion in the ear for near-threshold sound detection. Nat. Neurosci. **14**: 770. doi: 10.1038/nn.2827. PMID: 21602821.

Dannhof, B.J., Roth, B., and Bruns, V. 1991. Length of hair cells as a measure of frequency representation in the mammalian inner ear?. Naturwissenschaften. **78**: 570–573. doi: 10.1007/BF01134454. PMID: 1780010.

Dong, W., and Olson, E.S. 2009. In vivo impedance of the gerbil cochlear partition at auditory frequencies. Biophys. J. **97**: 1233–1243. doi: 10.1016/j.bpj.2009.05.057. PMID: 19720011.

Edge, R.M., Evans, B.N., Pearce, M., Richter, C.P., Hu, X., and Dallos, P. 1998. Morphology of the unfixed cochlea. Hear. Res. **124**: 1–16. doi: 10.1016/S0378-5955(98)00090-2. PMID: 9822898.

Fettiplace, R., and Kim, K.X. 2014. The physiology of mechanoelectrical transduction channels in hearing. Physiol. Rev. **94**: 951–986. doi: 10.1152/physrev.00038.2013. PMID: 24987009.

Gao, G., and Zhou, K. 1992. Fiber analysis of the optic and cochlear nerves of small cetaceans. *In* Marine mammal sensory systems. *Edited by* J.A. Thomas, R.A. Kastelein, and A.Y. Supin. Springer, New York. pp. 39–52. doi: 10.1007/978-1-4615-3406-8_2.

Ketten, D.R. 1992*a*. The cetacean ear: form, frequency, and evolution. *In* Marine mammal sensory systems. *Edited by* J.A. Thomas, R.A. Kastelein, and A.Y. Supin. Springer, New York. pp. 53–75. doi: 10.1007/978-1-4615-3406-8_3.

Ketten, D.R. 1992*b*. The marine mammal ear: specializations for aquatic audition and echolocation. *In* The evolutionary biology of hearing. *Edited by* D.B. Webster, A.N. Popper, and R.R. Fay. Springer, New York. pp. 717–750. doi: 10.1007/978-1-4612-2784-7_44.

Ketten, D.R. 1997. Structure and function in whale ears. Bioacoustics. **8**: 103–135. doi: 10.1080/09524622.1997.9753356.

Ketten, D.R. 2000. Cetacean ears. *In* Hearing by whales and dolphins. *Edited by* W.W.L. Au, A.N. Popper, and R.R. Fay. Springer-Verlag, New York. pp. 43–108. doi: 10.1007/978-1-4612-1150-1_2.

Ketten, D.R., and Wartzok D. 1990. Three-dimensional reconstructions of the dolphin ear. *In* Sensory abilities of cetaceans. *Edited by* J.A. Thomas and R.A. Kastelein. Springer, New York. pp. 81–105. doi: 10.1007/978-1-4899-0858-2_6.

Lee, H.Y., Raphael, P.D., Xia, A., Kim, J., Grillet, N., Applegate, B.E., Bowden, A.K.E., and Oghalai, J.S. 2016. Two-dimensional cochlear micromechanics measured in vivo demonstrate radialtuning within the mouse organ of Corti. J. Neurosci. **36**: 8160–8173. doi: 10.1523/JNEUROSCI.1157-16.2016. PMID: 27488636.

Lei, R., Xie, H., Wang, J., Leppäranta, M., Jónsdóttir, I., and Zhang, Z. 2015. Changes in sea ice conditions along the Arctic Northeast Passage from 1979 to 2012. Cold Reg. Sci. Technol. **119**: 132–144. doi: 10.1016/j.coldregions.2015.08.004.

Lim, D.J. 1986. Functional structure of the organ of Corti: a review. Hear. Res. **22**: 117–146. doi: 10.1016/0378-5955(86)90089-4. PMID: 3525482.

Liu, Y., Gracewski, S.M., and Nam, J.H. 2015. Consequences of location-dependent organ of corti micro-mechanics. PLoS ONE. **10**: e0133284. doi: 10.1371/journal.pone.0133284. PMID: 26317521.

Morell, M., and André, M. 2009. Ear extraction and fixation protocol. http://www.zoology.ubc.ca/files/Ear_extraction_and_fixation_protocol_UBC.pdf.

Morell, M., Degollada, E., Alonso, J.M., Jauniaux, T., and André, M. 2009. Decalcifying odontocete ears following a routine protocol with RDO®. J. Exp. Mar. Bio. Ecol. **376**: 55–58. doi: 10.1016/j.jembe.2009.05.005.

Morell, M., Lenoir, M., Shadwick, R.E., Jauniaux, T., Dabin, W., Begeman, L., Ferreira, M., Maestre, I., Degollada, E., Hernandez-Milian, G., and Cazevieille, C. 2015. Ultrastructure of the odontocete organ of Corti: scanning and transmission electron microscopy. J. Comp. Neurol. **523**: 431–448. doi: 10.1002/cne.23688. PMID: 25269663.

Morell, M., Brownlow, A., McGovern, B., Raverty, S.A., Shadwick, R.E., and André, M. 2017. Implementation of a method to visualize noise-induced hearing loss in mass stranded cetaceans. Sci. Rep. **7**: 41848. doi: 10.1038/srep41848. PMID: 28165504.

Ni, G., Elliott, S.J., and Baumgart, J. 2016. Finite-element model of the active organ of Corti. J. R. Soc. Interface. **13**: 20150913. doi: 10.1098/rsif.2015.0913. PMID: 26888950.

Pujol, R., Lenoir, M., Ladrech, S., Tribillac, F., and Rebillard, G. 1992. Correlation between the length of outer hair cells and the frequency coding of the cochlea. *In* Auditory physiology and perception. Advances in the biological sciences **83**. *Edited by* Y. Cazals, L. Demeny, and K. Horner. Pergamon Press, Oxford, UK. pp. 45–52.

Roth, B., and Bruns, V. 1992. Postnatal development of the rat organ of Corti II. Hair cell receptors and their supporting elements. Anat. Embryol. **185**: 571–581. doi: 10.1007/BF00185616. PMID: 1605368.

Roth, E.H. 2008. Arctic Ocean long-term acoustic monitoring: ambient noise, environmental correlates, and transients north of Barrow, Alaska. M.Sc. thesis, ProQuest Dissertations Publishing, University of California, San Diego, Calif.

Schweitzer, L., Lutz, C., Hobbs, M., and Weaver, S.P. 1996. Anatomical correlates of the passive properties underlying the developmental shift in the frequency map of the mammalian cochlea. Hear. Res. **97**: 84–94. doi: 10.1016/0378-5955(96)00063-9. PMID: 8844189.

Sensor, J.D., Suydam, R., George, J.C., Liberman, M.C., Lovano, D., Rhaganti, M.A., Usip, S., Vinyard, C.J., and Thewissen, J.G.M. 2015. The spiral ganglion and Rosenthal's canal in beluga whales. J. Morphol. **276**: 1455–1466. doi: 10.1002/jmor.20434. PMID: 26769322.

Solntseva, G. 2010. Morphology of the inner ear in mammals with different ecological peculiarities in ontogeny. Vestn. Zool. **44**: e-1. doi: 10.2478/v10058-010-0013-y.

Soons, J.A., Ricci, A.J., Steele, C.R., and Puria, S. 2015. Cytoarchitecture of the mouse organ of corti from base to apex, determined using in situ two-photon imaging. J. Assoc. Res. Otolaryngol. **16**: 47–66. doi: 10.1007/s10162-014-0497-1. PMID: 25348579.

Spicer, S.S., and Schulte, B.A. 1994. Differences along the place-frequency map in the structure of supporting cells in the gerbil cochlea. Hear. Res. **79**: 161–177. doi: 10.1016/0378-5955(94)90137-6. PMID: 7806478.

Tsuji, J., and Liberman, M.C. 1997. Intracellular labeling of auditory nerve fibers in guinea pig: central and peripheral projections. J. Comp. Neurol. **381**: 188–202. doi: 10.1002/(SICI)1096-9861(19970505)381:2<188::AID-CNE6>3.0.CO;2-#. PMID: 9130668.

Von Békésy, G. 1960. Experiments in hearing. McGraw-Hill, New York.

Wartzok, D., and Ketten, D.R. 1999. Marine mammal sensory systems. *In* Biology of marine mammals. *Edited by* J.E. Reynolds, and S.A. Rommel. Smithsonian Institution Press, Washington, D.C. pp. 117–175.

Wartzok, D., Popper, A.N., Gordon, J., and Merrill, J. 2003. Factors affecting the responses of marine mammals to acoustic disturbance. Mar. Technol. Soc. J. **37**: 6–15. doi: 10.4031/002533203787537041.

Wever, E.G., McCormick, J.G., Palin, J., and Ridgway, S.H. 1971*a*. The cochlea of the dolphin, *Tursiops truncatus*: general morphology. Proc. Natl. Acad. Sci. U.S.A. **68**: 2381–2385. doi: 10.1073/pnas.68.10.2381. PMID: 16591947.
Wever, E.G., McCormick, J.G., Palin, J., and Ridgway, S.H. 1971*b*. The cochlea of the dolphin, *Tursiops truncatus*: hair cells and ganglion cells. Proc. Natl. Acad. Sci. U.S.A **68**: 2908–2912. doi: 10.1073/pnas.68.12.2908. PMID: 5289233.
Wever, E.G., McCormick, J.G., Palin, J., and Ridgway, S.H. 1972. Cochlear structure in the dolphin, *Lagenorhynchus obliquidens*. Proc. Natl. Acad. Sci. U.S.A. **69**: 657–661. doi: 10.1073/pnas.69.3.657. PMID: 16591969.
Yarin, Y.M., Lukashkin, A.N., Poznyakovskiy, A.A., Meißner, H., Fleischer, M., Baumgart, J., Richter, C., Kuhlisch, E., and Zahnert, T. 2014. Tonotopic morphometry of the lamina reticularis of the guinea pig cochlea with associated microstructures and related mechanical implications. J. Assoc. Res. Otolaryngol. **15**: 1–11. doi: 10.1007/s10162-013-0420-1. PMID: 24165807.